LEGIBILITY NOTICE

A major purpose of the Technical Information Center is to provide the broadest dissemination possible of information contained in DOE's Research and Development Reports to business, industry, the academic community, and federal, state and local governments.

Although a small portion of this report is not reproducible, it is being made available to expedite the availability of information on the research discussed herein.

LA-UR -90-2679

Los Alamos National Laboratory is operated by the University of California for the United States Department of Energy under contract W-7405-ENG-36

LA-UR--90-2679

DE90 016611

TITLE: TEXTURE-INDUCED ANISOTROPY AND HIGH-STRAIN RATE DEFORMATION IN METALS

AUTHOR(S): S. K. SCHIFERL and P. J. MAUDLIN
X-3 N-6

SUBMITTED TO: EXPLOMET 90
UCSD
San Diego, CA

August 12-17, 1990

Los Alamos Los Alamos National Laboratory
Los Alamos, New Mexico 87545

TEXTURE-INDUCED ANISOTROPY AND HIGH-STRAIN RATE DEFORMATION IN METALS

S. K. SCHIFERL and P. J. MAUDLIN

Los Alamos National Laboratory
Los Alamos, New Mexico 87545

We have used crystallographic texture calculations to model anisotropic yielding behavior for polycrystalline materials with strong preferred orientations and strong plastic anisotropy. Fitted yield surfaces were incorporated into an explicit Lagrangian finite-element code. We consider different anisotropic orientations, as well as different yield-surface forms, for Taylor cylinder impacts of hcp metals such as titanium and zirconium. Some deformed shapes are intrinsic to anisotropic response. Also, yield surface curvature, as distinct from strength anisotropy, has a strong influence on plastic flow.

I. INTRODUCTION

Crystallographic texture is a property of increasing interest for a number of high strain-rate processes, including anti-armor designs. The peculiar behavior of textured materials has been exploited in a number of ways, from spin compensation in shaped-charge liners to desirable yield anisotropy in new materials.

"Texture" refers to the preferred orientation of single-crystal grains in a polycrystalline solid For hexagonal-close packed metals, such as titanium and zirconium, plastic anisotropies

due to texture can be very large. Yield anisotropies can be > 2:1 [1], and plastic strain ratios (R-values) typically range from 3 to 7 [2]. For cubic metals, yield anisotropies tend to be small, but strain anisotropies can be significant (R ~ 0.6 for rolled copper; R > 2.5 for some steels) [2]. A strong preferred orientation is typically the result of large deformation (> 50%); the patterns of deformation textures depend on both crystal structure and deformation path.

We have previously modeled changes in texture and corresponding changes in yield anisotropy during liner collapse in titanium shaped-charge jets [3], a system where inertial effects dominate the flow. In the present study, we investigate the role of texture in a different kind of system – a high-strain-rate regime where inertial effects no longer dominate. Examples of this kind of system include the Taylor anvil test (end-on impact of a cylinder on a flat target) and EFPs (explosively-formed penetrators: collapse of a metal liner to a stable shape). Both systems are known to be sensitive to material properties, particularly details of the yield strength. The simulation of anisotropic effects in this class of problem requires a coupled approach: the deviatoric stress states encountered by the material have a significant effect on the kinematics of the deformation, and these stress states need to be part of the yield function.

We will concentrate on appropriate constitutive relations for Taylor impacts of anisotropic cylinders. For such a moderate strain deformation, we assume constant anisotropy (constant yield-surface shape) as a first approximation. The scale of the yield surface will not, in general, remain constant; strain hardening, strain-rate hardening, and thermal softening change the overall yield within much smaller strains than texture evolution changes the anisotropy. We also assume that our material has inhibited twinning; this subject is discussed in more detail in Sec. IV.

Determining the shape of the yield function is more complex. An anisotropic yield function is, by its nature, directional. Ideally, our data would include probes of the material with many different stresses. In practice, we have at most a few yield measurements and/or R-values, plus some constitutive rules for the isotropic case. In this situation, texture calculations, which model the underlying cause of single-phase anisotropy, can be useful. A texture code [3] "samples" an oriented collection of grains by applying a strain tensor; deformation of each grain is via the single-crystal mechanisms of slip and twinning. We consider the activation of any deformation system to require a certain critical-resolved-shear-stress (CRSS); the stress on each grain is the sum of the CRSSs for the active systems. To calculate yield surface points, critical stresses are averaged over the grains. A fitting function for the stress points and the modifications required for the continuum code are described in Sec. II, along with an orthogonal representation introduced to help visualize and fit the yield surface.

In the present work, we investigate the effect of large plastic anisotropy for Taylor cylinder tests. The material properties are typical of α-titanium (hcp) and some of its alloys, with twinning inhibited. We consider features of the deformed shapes, for anisotropic orientations $\beta = 0°, \pm 45°, 90°$ (where β is the initial angle between the material's weak axis and

the cylinder axis), and for different curvatures of the yield surface. The anisotropic simulations exhibit significant differences from isotropy, particularly for ß = ± 45°, where shear-strengthening (or shear-weakening) produce shapes specific to anisotropic response. The results also indicate that anisotropic response is strongly influenced by yield-surface curvature, rather than merely by the strength anisotropy that determines yield-surface eccentricity.

II. MODELING PLASTIC ANISOTROPY

To use texture information for a constitutive model, we need to generate a yield surface. As described above, a textured yield surface is a collection of stress points, not an analytic function. We need to find a function that reproduces the main features of the point distribution, but does not incorporate detail that a continuum simulation cannot resolve. We use the texture code only for the shape of the yield surface, not the scale; we normalize the yield surface by applying the texture code to a randomly oriented collection of grains. We also note that a general texture code requires no special symmetry, and is therefore adaptable to 3D simulations. For simplicity we consider axisymmetric cases, which can be addressed with 2D codes.

To visualize and fit the yield surface, we introduce a 3D stress space. For a 2D simulation, there are three independent components of the deviatoric stress tensor: two diagonal components and one off-diagonal component. We refer to the orthogonal set {Sx, Sy, Sz}, with Sx and Sy in the pi-plane, the plane in which the diagonal deviatoric stresses are at 120° to each other. One possible linear combination of tensor components is:

$$Sx = -\sqrt{3}\left(\frac{1}{2}S_{11} + S_{22}\right);\quad Sy = \frac{3}{2}S_{11}\quad ;\quad Sz = \sqrt{3}\,S_{12}\quad . \qquad (1)$$

This representation has a number of advantages. It allows for easy fitting of a yield function, and easy visualization of stress paths on the yield surface. It also allows for translation, to accommodate unequal yield strengths in tension and compression (a significant feature of many materials when twinning is involved). A spherical yield surface corresponds to isotropy, and an ellipsoidal yield surface, without translation, corresponds to Hill's [4] quadratic surface.

The characteristic features of the yield surface for a particular material depend heavily on the crystal symmetry, as well as the grain orientation distribution. Figures 1-2 show projections of the polycrystalline yield surface on the pi-plane for two cases: a compression texture for hcp crystals (α-titanium) [2] and a rolling texture for fcc (copper) [5]. Neither form suggests a simple shape: the former resembles a flattened ellipse, the latter a faceted border.

A useful form for an hcp yield surface is the superquadric function [6]:

$$F = \left[\left(\left(\frac{Sx - b_1}{a_1} \right)^{2/\varepsilon_2} + \left(\frac{Sy - b_2}{a_2} \right)^{2/\varepsilon_2} \right)^{\varepsilon_2/\varepsilon_1} + \left(\frac{Sz - b_3}{a_3} \right)^{2/\varepsilon_1} \right]^{\varepsilon_1} - 1 \quad , \qquad (2)$$

where a_1, a_2, a_3 define the eccentricity; b_1, b_2, b_3 are offsets in the x, y, z directions; and ε_1 and ε_2 are curvature parameters in the polar and azimuthal directions. This form gives a smooth function, and can fit 3D shapes ranging from a needle to an ellipsoid to a box. As Fig.1 indicates, a superquadric fits the hcp yield surface much better than a simple ellipsoid.

The fcc yield surface presents a problem. A superquadric function has the wrong symmetry, and a fit will also tend to smooth out the vertices. However, we can reproduce some salient features of an fcc yield surface – the flat spots and vertices – by choosing superquadric parameters to fit a box-like shape. The box (see Fig.3d) is globally incorrect, but can give us some insight into the effect of a faceted yield surface on plastic deformation.

Finally, to use these yield surfaces it is necessary to make several major modifications to a continuum code. First, we evaluate the constitutive relations in a reference material frame, and use explicit rigid-body rotations to connect laboratory and material frames. The necessary rotation matrix is obtained from the polar decomposition of the deformation gradient tensor [7]. Also, we use an associative flow algorithm [8] to update the stresses. If the stress state is plastic, associative flow guarantees a plastic strain normal to the yield surface.

III. PROCEDURE

Our method, to calculate high-strain-rate response for anisotropic materials, is based on a yield function with a constant anisotropic shape, incorporated into a continuum code. Taylor cylinder tests were simulated with a modified version of EPIC2-88 [9], an explicit Lagrangian 2D finite-element code. The cylinders were 1-inch long, with an L/D of 10/3. The initial velocity was 190 m/s.

Our anisotropic material was modeled from the general features of heavily cross-rolled (transversely isotropic) titanium or zirconium sheet [10]; this sheet gives an R value of 9, which corresponds roughly to an anisotropy ratio of $z/x \sim 2.25$, where z is the compressive yield in the through-thickness direction and x is the average compressive yield in the plane of the sheet. Details of the yield surface, including shear strengths, were obtained with a texture simulation, using single-crystal properties of hcp titanium at moderate temperatures and relatively high strain-rates. The details of the nontwinning texture calculation have been described elsewhere [3]; here we use a CRSS of 3 for the secondary slip systems. Hardening and thermal softening were approximated by a rate-dependent constitutive model [11]. Since

our main interests in these simulations concern systems with large plastic strains, we treat elastic response simply as isotropic.

Several different yield surfaces were constructed for these calculations; their 3D representations are shown in Figs. 3a-d. The parameters, in terms of a normalized superquadric function (compare Eqn. 2) are as follows:

1) Isotropic: $a_1 = a_2 = a_3 = 1$, $\varepsilon_1 = \varepsilon_2 = 1$
2) Ellipsoidal model, using the strength anisotropies as major and minor axes (a_3 is the shear strength): $a_1 = 0.57$, $a_2 = 1.16$, $a_3 = 1.08$, $\varepsilon_1 = \varepsilon_2 = 1$
3) Superquadric fit: $a_1 = 0.57$, $a_2 = 1.16$, $a_3 = 1.08$, $\varepsilon_1 = 0.75$, $\varepsilon_2 = 0.76$
4) Cubical superquadric, to evaluate the effect of corners on an otherwise isotropic yield function: $a_1 = a_2 = a_3 = 1$, $\varepsilon_1 = \varepsilon_2 = 0.1$

The simulations were performed for the orientations $\beta = 0°, \pm 45°$, and $90°$, where β is the angle between the material weak axis and the cylinder axis.

IV. RESULTS AND CONCLUSIONS

The deformed shapes from simulations of anisotropic and isotropic Taylor cylinder impacts are shown in Figs.4–5. For Fig.4, we have used an anisotropic yield surface corresponding to the standard ellipsoidal form. For $\beta = 0°$, the weak direction is along the cylinder axis; this orientation realized the most compressive strain. For $\beta = \pm 45°$, the profiles in both cases are qualitatively different than the isotropic results, and the differences are large; the special nature of anisotropic response can maximize or minimize resistance to shear. Practically, orientation $\beta = 90°$ could be cut from a thick cross-rolled billet and $\beta = 0°$ from an extrusion. Diagonal cuts from the billet could give $\beta = \pm 45°$, but only in one plane; complete profiles of such cylinders are part of a 3D problem, and beyond the scope of the present study.

The cylinder profiles from a superquadric function, including a fit to the textured yield surface, are shown in Fig.5. The differences from isotropy are actually smaller than for the ellipsoidal surface, even though the yield anisotropies are the same in both cases. Some insight into these differences can be obtained by constructing deviatoric stress paths on the yield surfaces for particular computational cells. Figures 3a-c show these paths for the isotropic, ellipsoidal, and superquadric models, for $\beta = 0°$, and for a cell near the edge of the cylinder toe. It is clear that the anisotropic paths differ from the isotropic path. What is more striking is the amount of time spent near parts of the surfaces with high curvature. It is the lower curvature in the superquadric that appears to modify the effects of anisotropy.

This effect can be described as an "attraction" of stress states to regions of high curvature [12]. That the "attraction" is due to curvature, not eccentricity, can be seen in Fig.3d, which shows the stress path for a cubical yield surface with slightly rounded corners. Figure 5 includes the final cylinder profile for this yield surface; the differences from isotropy are large, and qualitatively different than for the other anisotropic functions. This behavior has important implications for the behavior of highly-textured cubic materials, particularly for fcc metals like copper and aluminum, where yielding behavior exhibits minimal yield strength anisotropy but suggests flat spots and vertices.

It should be noted that these curvature effects are seen only with associative flow [12], where the plastic strain is normal to the yield surface. Nonassociative flow laws (e.g., radial return on a nonspherical surface) and anisotropic models with spherical yield surfaces (kinematic hardening) will not produce these effects.

The major discrepancy in this modeling is the absence of any texture (and yield surface shape) change. Gradual evolution, from unequal grain rotations due to slip, is probably not the major difficulty here; the Taylor cylinder strains, except perhaps at the edge of the toe, are typically < 30%. Also, while texture does change with deformation, the yield anisotropy changes more slowly. A more serious problem is the possibility of deformation twinning.

For many hcp materials, and for some deformation modes (particularly tension in the strong direction), twinning can effectively "flip" a texture within a strain of only a few percent. For simplicity, we have assumed that twinning is inhibited. This is possible for a number of alloys, for very small grain size, for certain initial dislocation structures, and for materials with certain impurities [13]. For an hcp material where twinning does operate, the $\beta = 0°$ orientation would be affected: compression in the weak direction would effectively rotate the anisotropy, making the deformation along the axis and in the toe less extreme. For such materials, and for large deformations, the effects of texture evolution need to be addressed.

We have concentrated here on the effects of plastic anisotropy on high-strain-rate deformation. For moderate strains such effects can be large – and are not amenable to isotropic treatments. Our simulations show that the major effects stem from differences in the stress paths, including attraction to regions of high curvature on anisotropic yield surfaces. To model such behavior, it is necessary to have detailed information about yielding behavior. Texture studies, as a prescription for yield surface models, can help provide insight into this difficult area of constitutive modeling.

ACKNOWLEDGMENTS

This work was supported by the Defense Advanced Research Projects Agency, and through the Joint DoD/DOE Munitions Technology Development Program.

REFERENCES

1. R. G. Ballinger and R. M. Pelloux, *J. Nucl. Mater.*, 97:231 (1981).
2. W. F. Hosford and R. M. Caddell, *Metal Forming: Mechanics and Metallurgy*, Prentice-Hall, Englewood Cliffs, New Jersey, 1983.
3. S. K. Schiferl, *J. Appl. Phys.*, 66:2637 (1989); S. K. Schiferl, in *Shock Compression of Condensed Matter* - 1989 (1990).
4. G. R. Canova, V. F. Kocks and C. N. Tome, *J. Mech. Phys. Solids*, 33:371 (1985).
5. R. Hill, *The Mathematical Theory of Plasticity*, Oxford University Press, London, 1950.
6. F. Solina and R. Bajcsy, *IEEE Trans. Pat. Anal. Mach. Intell.*, 12:131 (1990).
7. J. K. Dienes, *Acta Mech.*, 32:217 (1979). For implementation, see: D. P. Flanagan and L. M. Taylor, *Comp. Meth. Appl. Mech. Eng.*, 62:305 (1987).
8. R. Hill, *Plasticity*, Clarendon Press, Oxford, 1956.
9. G. R. Johnson and R. A. Stryk, Air Force Armament Lab. Report TR-86-51 (1986).
10. F. Larson and A. Zarkades, Metals and Ceramics Inf. Center Report 74-20 (1974).
11. G. R. Johnson and T. J. Holmquist, Los Alamos Report LA-11463-MS (1989).
12. T. J. R. Hughes, in *Proc. of the Workshop on the Theoretical Foundations for Large-Scale Computations of Nonlinear Material Behavior* (1984).
13. H. Conrad, *Prog. Mater. Sci.*, 26:123 (1981).

FIG. 1 *Deviatoric pi-plane yield locus for a (twinning) titanium compression texture. Note unequal yields in tension and compression. Points are from texture calculations. Lines are analytic forms.*

FIG. 2 *Deviatoric pi-plane yield locus for rolled copper, 85 % reduction (from Ref. 4). Texture calculation.*

FIG. 3 *Yield surfaces and deviatoric stress paths for Taylor cylinder impacts, $\beta = 0°$, in a 3D representation (see Sec. II). β is the initial angle between the material weak axis and the cylinder axis.*

FIG. 4 *Taylor cylinder profiles, using an ellipsoidal yield surface (β is defined in Fig. 3). The abscissa is expanded to show detail.*

FIG. 5 *Taylor cylinder profiles, using a superquadric yield surface, $\beta = 0°$ (β is defined in Fig. 3). The abscissa is expanded to show detail.*

Draft

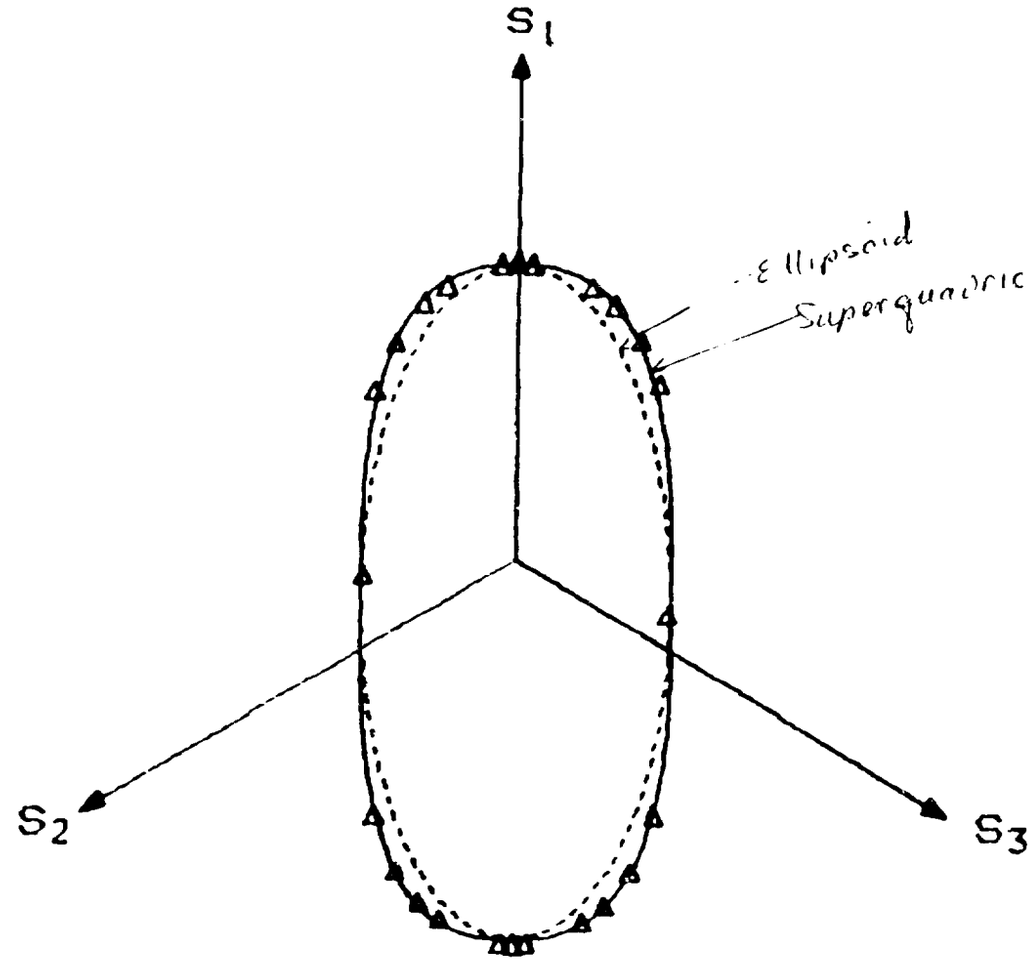

Fig 1

→ Maudlin 8/2/90

Draft

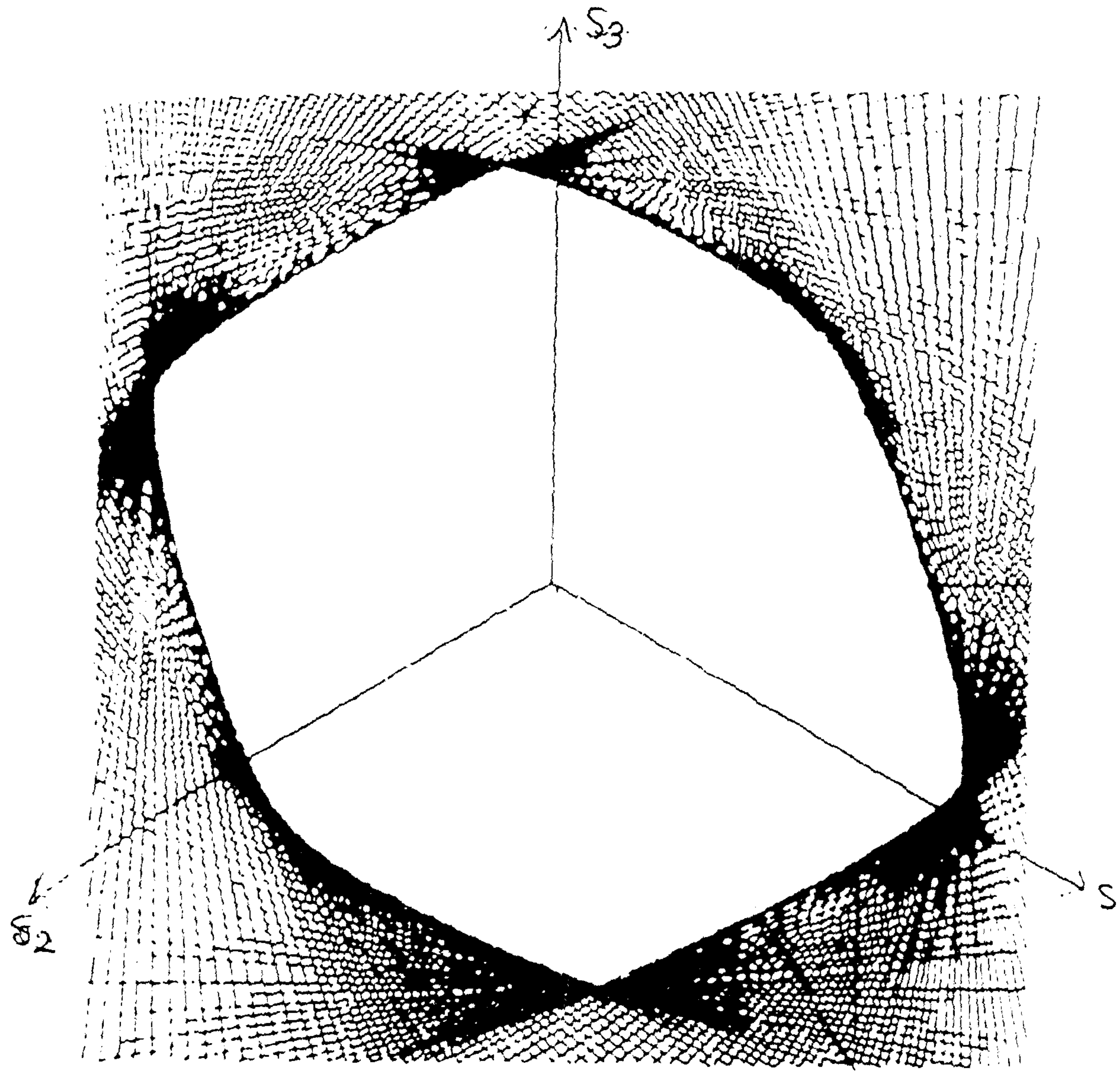

Fig. 2

J. Schafer + P. Naudlen 8/2/90

Draft

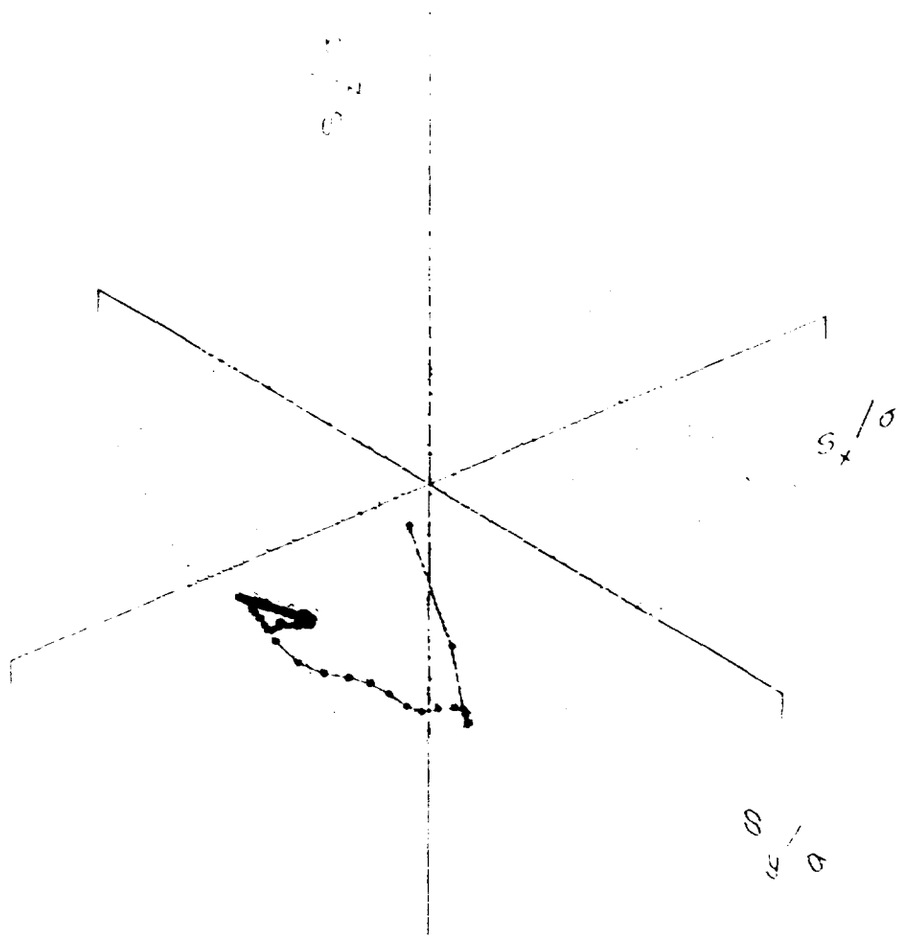

a) Isotropic

Fig 3a

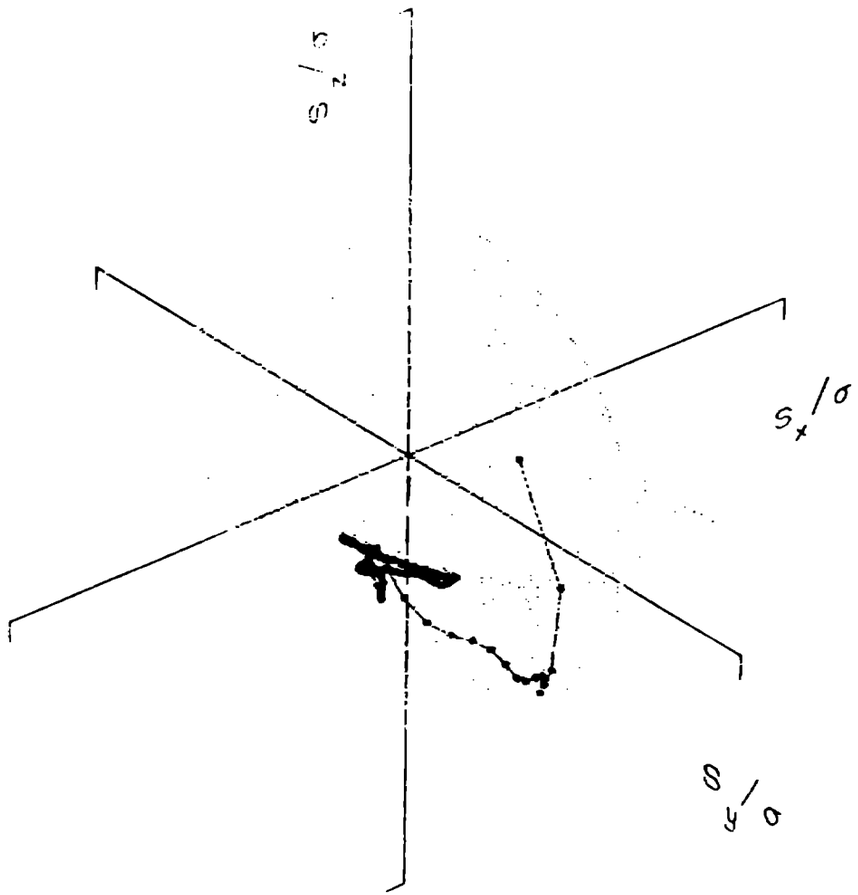

b) Ellipsoid

Draft

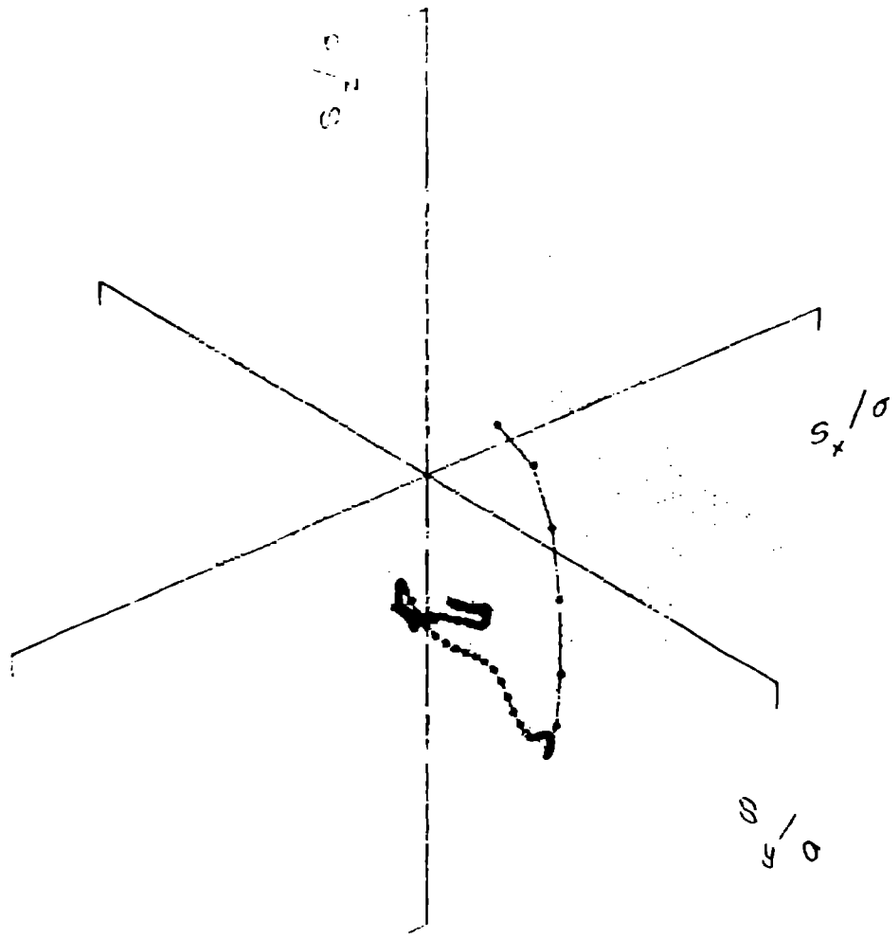

a) Superquadric titanium

Fig 30.

b) Cubic and c) Hexagonal steels

Draft

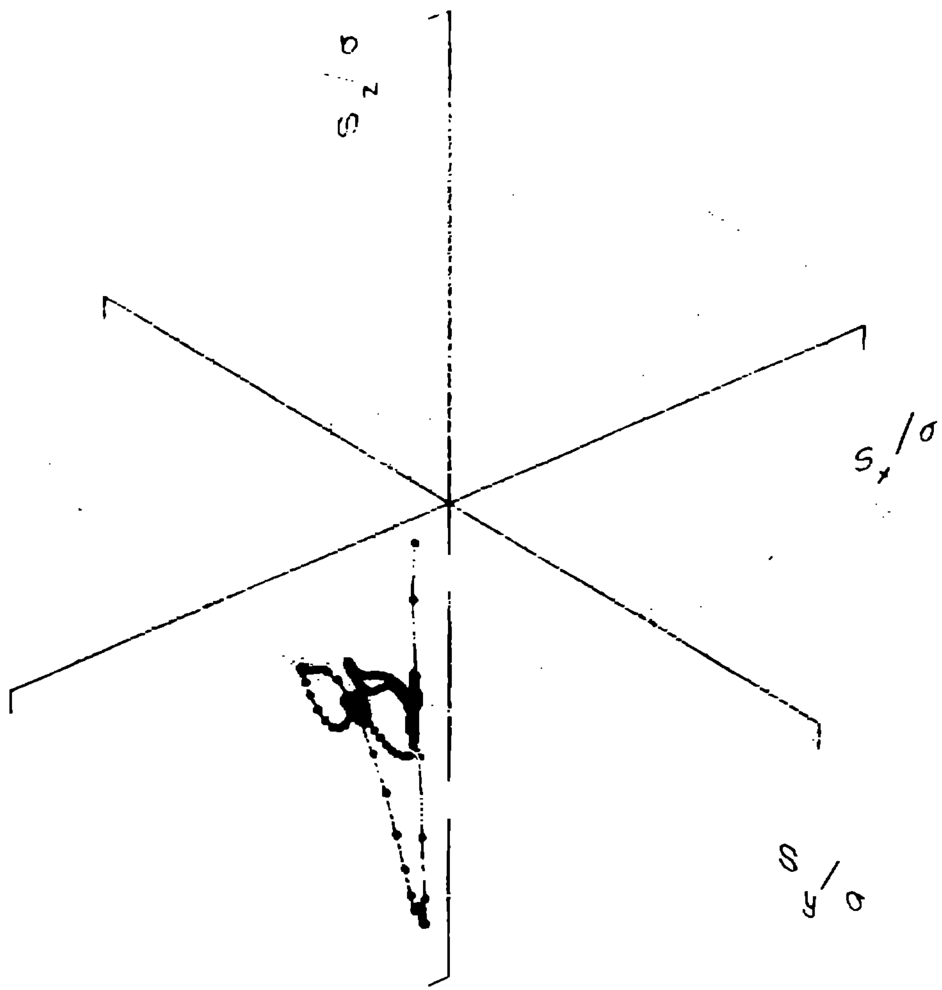

d) Superquadric cube

Fig 3d
C. Liefer and P. Mandler [illegible]

Draft

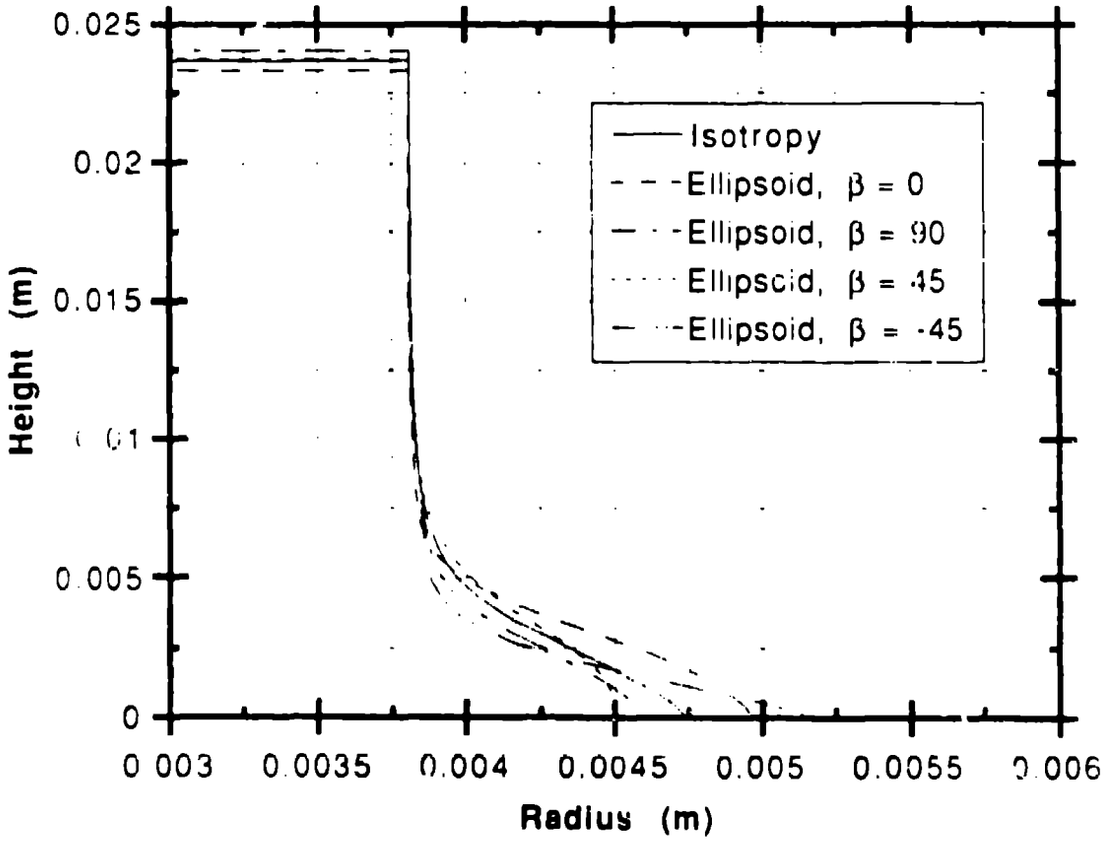

Fig 4

[illegible] 8/2/90

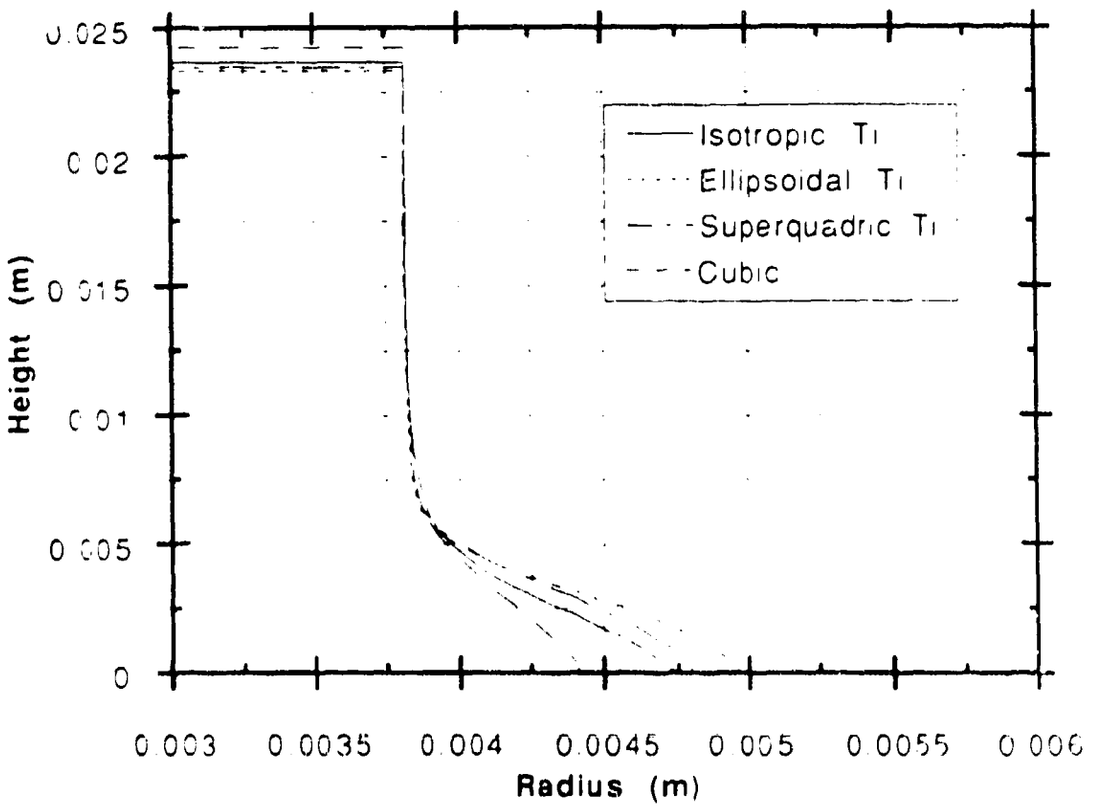
0.025
0.02
0.015
0.01
0.005
0
Height (m)
0.003
0.0035
0.004
0.0045
0.005
0.0055
0.006
Radius (m)
Isotropic Ti
Ellipsoidal Ti
Superquadric Ti
Cubic